BIOCHEMISTRY
including biophysical chemistry & molecular biology

Article

pubs.acs.org/biochemistry

Solvent-Dependent Gating Motions of an Extremophilic Lipase from *Pseudomonas aeruginosa*

Quentin R. Johnson,[†,‡] Ricky B. Nellas,[‡,§] and Tongye Shen*[,‡,§]

[†]UT-ORNL Graduate School of Genome Science and Technology, Knoxville, Tennessee 37996, United States
[‡]Center for Molecular Biophysics, Oak Ridge National Laboratory, Oak Ridge, Tennessee 37830, United States
[§]Department of Biochemistry and Cellular & Molecular Biology, University of Tennessee, Knoxville, Tennessee 37996, United States

ABSTRACT: Understanding how organic solvent-stable proteins can function in anhydrous and often complex solutions is essential for the study of the interaction of protein and molecular immiscible interfaces and the design of efficient industrial enzymes in nonaqueous solvents. Using an extremophilic lipase from *Pseudomonas aeruginosa* as an example, we investigated the conformational dynamics of an organic solvent-tolerant enzyme in complex solvent milieux. Four 100-ns molecular dynamics simulations of the lipase were performed in solvent systems: water, hexane, and two mixtures of hexane and water, 5% and 95% (w/w) hexane. Our results show a solvent-dependent structural change of the protein, especially in the region that regulates the admission of the substrate. We observed that the lipase is much less flexible in hexane than in aqueous solution or at the immiscible interface. Quantified by the size of the accessible channel, the lipase in water has a closed-gate conformation and no access to the active site, while in the hexane-containing systems, the lipase is at various degrees of open-gate state, with the immiscible interface setup being in the widely open conformation ensembles. The composition of explicit solvents in the access channel showed a significant influence on the conformational dynamics of the protein. Interestingly, the slowest step (bottleneck) of the hexane-induced conformational switch seems to be correlated with the slow dehydration dynamics of the channel.

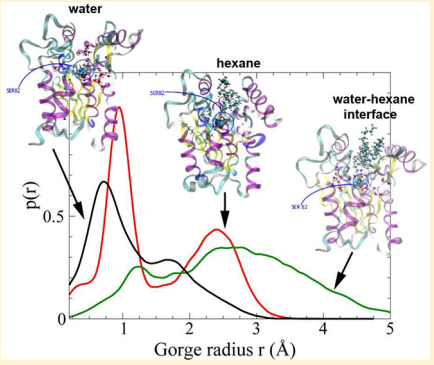

The structural stability of proteins involves a delicate balance between the favorable internal interaction among residues of the protein and the protein−solvent interaction. Many proteins optimize their structural stability in an aqueous environment.[1] When submerged in organic solvents or placed at immiscible interfaces, their native structures are likely to be weakened and their activities diminished. But for a few families of proteins that interact directly with an organic substrate (at the interface), the desired reaction environment may be more complicated. For some of these biomolecules, their functions are kept in a seemingly anhydrous environment due to the presence of a small amount of hydration water.[2] However, there are exceptional natural proteins, from surfactins[3] to lipases,[4,5] that operate efficiently in a water−oil interface or in organic solvents, especially some enzymes of microbial origin that thrive in deep-sea mud.[6] These proteins are structurally stable and biosynthetically active at an organic solvent interface.

In this work, we focus on one such important extremophilic enzyme, a lipase from *Pseudomonas aeruginosa*, which is inactive in an aqueous milieu and activated at the water−oil immiscible interface.[4,7,8] Lipases are proteins that assist in the forming and breaking of ester bonds of glycerol esters.[9,10] They are known to play important roles in biochemical pathways, such as transport processes and stereoselective biotransformations.[10] Besides these natural biological functions, lipases have a diverse set of industrial applications, from the break down of unwanted oily components of cosmetics, detergents, and waste to the synthesis of esters.[11]

Lipases belong to the superfamily of α/β-hydrolase,[9] a group of enzymes (including proteases, esterases, lipases, and peroxidases) sharing the same α/β fold.[12] At the active site, these enzymes share the catalytic triad motif for breaking covalent bonds. Apparently, this well-studied enzymatic mechanism is quite efficient once the substrate reaches the active site.[9] The discerning factor among hydrolases is substrate selectivity, which begins at the precatalytic step. The concealed catalytic cavity and the switchable gate enable conformational control of ligand admission.[12,13] Indeed, lipases obtained from different species, from fungus (*Candida antarctica*) to bacterium (*Burkholderia cepacia*), share this canonical fold and the catalytic triad.[14,15] As shown in Figure 1a, the lipase from *P. aeruginosa* folds with its active site buried at the center. There is a 15 Å long gated channel that leads to the ovoid shaped active site cleft.[16] The main feature of this hydrophobic channel is the "lid" region that regulates entry of substrates and solvent molecules to the gorge. Movement in this region is critical for the enzyme activity.[16]

A plethora of crystal structures of different lipases at various binding states have been reported in an effort to understand

Received: April 30, 2012
Revised: July 9, 2012
Published: July 25, 2012

   dx.doi.org/10.1021/bi300557y | *Biochemistry* 2012, 51, 6238−6245

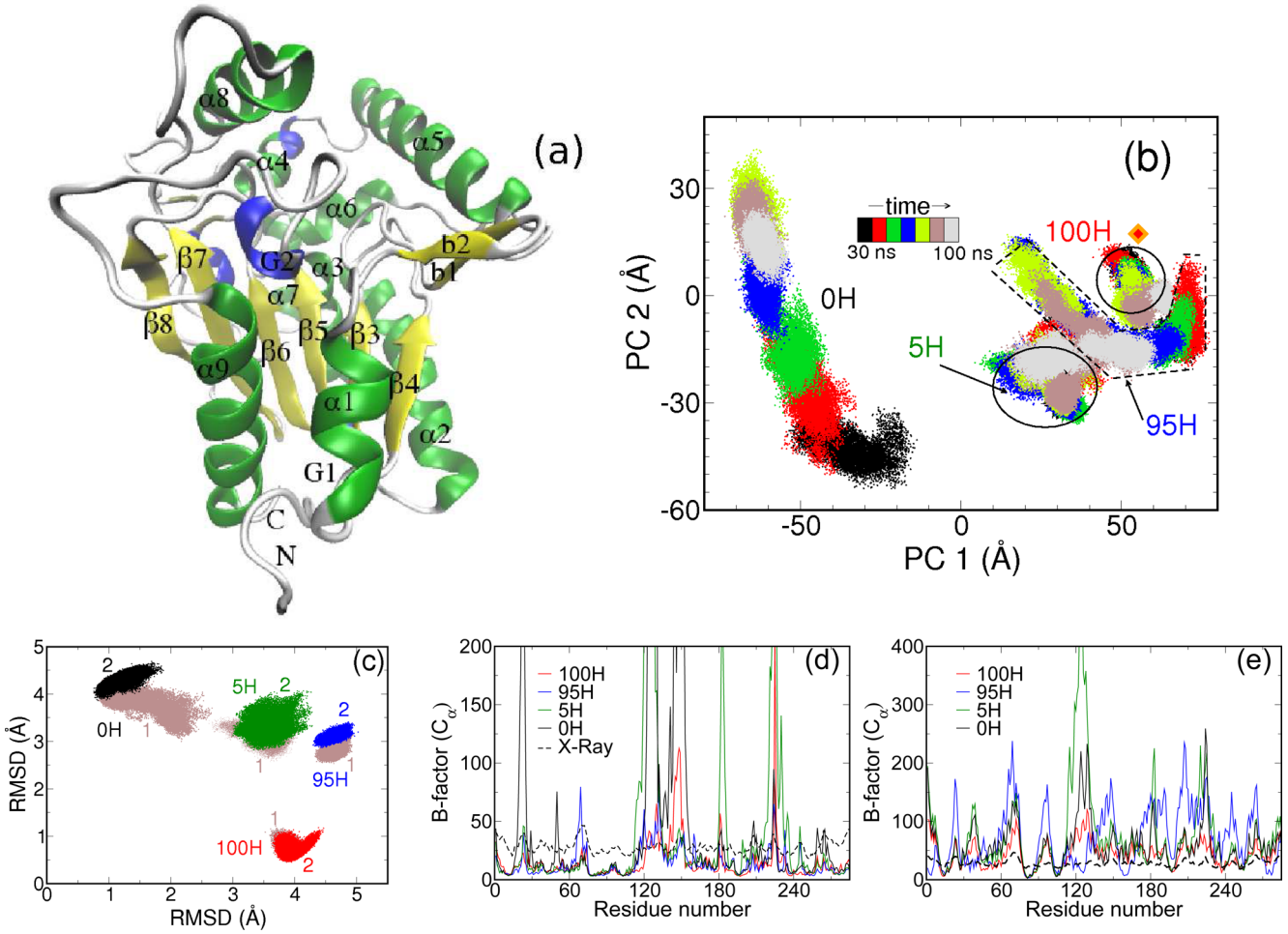

Figure 1. (a) 1EX9 canonical view with structural elements labeled. (b) Principal component analysis (PCA) for the lipase in respective solvent conditions. PC1 and PC2 are the top two principal components (PCs), respectively. Each color block is 10 ns of data. The diamond symbol (orange) indicates the location of the original crystal conformation projected on these two PCs. (c) 2D-rmsd plot of the lipase in various solvent conditions: 100H (red), 95H (blue), 5H (green), and 0H (black). The *x*-axis (*y*-axis) indicates the rmsd of the snapshots from the mean structure of the lipase in water (hexane). Labels 1 and 2 represent the first and second half of the final 70 ns of the simulations, respectively. Cα B-factor of the lipase in various solvent conditions: 100H, 95H, 5H, 0H, and X-ray (dashed line) for the last 100 ns (d) and 10 ns (e) of data. Color notation is identical to that of (c).

how this channel operates.[15−21] They reveal that this channel exists in different conformational states. The ligand-bound form is often associated with the channel being relatively wide open (open state), while the apo form of the lipase presents a closed channel without ligand access (closed state). Several aspects of this conformational gating mechanism are still missing. First, it is important to provide an ensemble view of probable states of the conformation of the access channel throughout the gating motion, not just the qualitative description of dichotomous states (open vs closed). Second, the mechanism of opening and closing the channel is solvent-sensitive, and it is important to study the conformational dynamics at realistic complex solvent interfaces.

Computational studies on the aforementioned lipases in solution have also been carried out to obtain insight into how the solvent facilitates the conformational shifts of lipases.[14,22−30] Several molecular dynamics simulations have discovered important motions of lipases, especially the movement of the gate triggered by the hydrophobicity of the environment.[22] To our knowledge, all previous simulations of lipases are about 35 ns or much less. As shown in a previous study[14] and in the results presented in this work, it may take lipases as long as 30 ns to repel water molecules inside the gorge and to make the conformational switch to close the gate. Thus, longer time scale simulations are required to get better statistics. A more quantitative analysis of the gated access channel (as opposed to the open/closed binary description of the end points) will facilitate a comparison of the conformation ensemble in a more precise manner, as we will illustrate below using the gorge radius analysis.

Several studies on how the open-close conformational switch of lipases may work in various solvent systems have been reported. For *Burkholderia cepacia* lipase (BcL), when in aqueous solution, an initially open conformation gradually closes. Conversely, when in toluene (also in octane or water-octane (50/50) interface[25]), an initially closed BcL opens gradually.[14] For *Bacillus sp.* (Lip42), in pure water and in 100% dimethyl sulfoxide (DMSO), the access channel seems to be unperturbed, while in 60% (v/v) DMSO distortion of conformations (accompanied by formation of nonnative H-bonds) is observed.[26] For *P. aeruginosa* (PAO1), when in water, an initially open structure becomes closed and starts to open again when moved to a water−octane (50/50) interface.[22] Note that all of these previous studies are performed either in a

dx.doi.org/10.1021/bi300557y | *Biochemistry* 2012, 51, 6238−6245

pure solvent or a relative "bulky" immiscible interface, such as the water−octane (50/50) interface. The effect of the presence of a small amount of water or organic moiety in the solvent mixture on the conformational transitions of the lipase is much less examined. Most practical interfaces encountered by lipases may not be an ideal case. Rather, we are interested in less well-formed molecular interfaces with a small number of organic solvent molecules surrounded by water or vice versa. Such setups (with less surface area between the immiscible interface) carry less perturbation due to surface tension energy and thus minimizes the effects of bulky interface.

Lipase from *P. aeruginosa* (PAL) strain LST03 has already been characterized in terms of sequence and activity.[6,31,32] It has been reported to show unusual stability and activity in organic solvent systems. The succeeding discussions will focus on the statistical analysis of the gating motion of the lipase in four water−hexane solvent compositions and the role of gorge solvent molecules on the conformational dynamics of the protein.

SYSTEMS AND METHODS

Using the lipase from *P. aeruginosa*, we performed a series of molecular dynamics simulations in four explicit water−hexane solvent environments: 100% hexane, 95% hexane, 5% hexane, and 0% hexane (pure water). For convenience, these four systems are labeled as "100H", "95H", "5H", and "0H", respectively. Although the sequence of PAL-LST03 is known, its crystal structure is not yet available. Thus, we turn to its relative, the lipase from *P. aeruginosa* (PAO1). This lipase has 285 residues and its crystal structure has been reported in protein data bank as PDB ID: 1EX9.[16] It only differs from PAL-LST03 by a single residue (a very subtle change of 1EX9:Val^{130} to Ile in helix α5). A separate study demonstrated that this substitution does not affect the conformations of the peptide (α5 region) in different solvent conditions (data not shown).

The crystal structure PDB: 1EX9[16] (with ligand removed) was used as the starting structure for all simulations. Systems were prepared using the xleap module in AMBER 10.[33] AMBER 99SB force field was used for the protein while TIP3P[34] was used for water. The organic solvent hexane was modeled using the antechamber module of AMBER 10.[33] For the construction of the 0H system, the protein is immersed in a periodic box containing 10 465 water molecules. For the 100H system, the protein is solvated in 2175 hexane molecules. The initial state of the 5% (4.86%) hexane mixture (5H) system was constructed by first solvating the protein with 113 hexane molecules and then adding 10 591 water molecules on the outer layer. The initial state of the 95% (95.23%) hexane mixture (95H) system was constructed by first solvating the protein with 200 water molecules then adding 836 hexane molecules on the outer layer. Finally, three sodium ions were added to neutralize each system.

The presence of a tightly bound calcium ion is critical to the structural integrity of the lipase. The coordinated metal ion (Ca^{2+}/Zn^{2+}) enhances the thermostability of the protein and its absence causes major structural changes.[19,27,28] For PAO1, Ca^{2+} stabilizes the loop containing His^{251}, a part of the catalytic triad.[16] Since the metallic bonding aspect of the calcium is difficult to incorporate, we simply fix the positions of calcium and the four neighboring oxygens (Asp^{209}:O, Asp^{253}:O, Gln^{257}:O, Leu^{261}:O) using the protocol described in NAMD2.7.[35]

For each system, minimization, heating, and equilibration (for approximately 10 ns) were conducted and followed by a 100 ns molecular dynamics production run using NAMD2.7 package.[35] Simulation pressure and temperature are kept constant at 1.01325 bar and 300 K, respectively. Langevin thermostat is used to regulate temperature. Long-range interactions are treated using the particle mesh Ewald method. All bonds involving hydrogen atoms are constrained using the SHAKE algorithm. A time step of 2 fs is used to integrate the equations of motion. Frames are collected at 1 ps intervals. Data collected from the 10 ns equilibration run were disregarded and analysis was performed on the final 100 ns molecular dynamics production data.

The program HOLE[36] was used here to probe the gorge radius of the lipase. This software has been routinely employed to measure the size of ion channels and cavities of protein structures.[36−38] We performed the analysis on each snapshot and obtained a global measurement of the openness of the access channel that leads to the active site. This procedure does not measure a particular distance between arbitrarily defined parts of the channel. Rather, it gives the size of the bottleneck of the channel, which is dependent on the snapshots. This method requires an input of atomic coordinates, the point of origin of the gorge (cpoint), and a defined gorge direction (cvect).[36] A library of atomic radii is included in the HOLE program and was used to construct the geometry of the protein surface. For each conformation of the lipase, HOLE is able to calculate the effective size of the channel as a function of the semiautomatic found path, $\rho(\vec{r})$. The path is a set of coordinates linked from the active site to the entrance. We then further defined the minimum radius along this path as the bottleneck.

The two crucial factors for this probe are the cpoint and cvect. We first calculated the center between four residues (Gly^{24}, Phe^{214}, Leu^{138}, and Phe^{117}) that surround the opening of the gorge in all cardinal directions. We then find the average position (cpoint) between this center point and the position of Ser^{82}. Similarly, the cvect originates at the cpoint and extends along the z axis toward the surface of the protein.

RESULTS AND DISCUSSION

As mentioned previously, the initial structure of the lipase for all simulations was that of the crystal structure complexed with a ligand (removed for this study) at the active site PDB: 1EX9.[16] This structure was deemed to represent an open and active conformation. Lipases are widely believed to be activated only at an oil−water interface.[14] Thus, we are interested in whether the lipase in each solvent condition will remain in the initial conformation or explore others, such as the closed conformation that features a closed channel with no ligand access. Practically, this closed conformation is associated with a constricted gate via the displacement of the α5 helix toward the α8 helix.[22] Thus, one particular interesting region is the α5 helix (residues 126−147) because the movement of this helix seems to govern the opening of the gate. We also pay attention to α8 (residues 210−222) because it has previously been proposed to affect the gating mechanism as the second lid.[22] Another important aspect of this work is the solvent analysis as we will relate the dynamic motion of the protein to that of the solvent molecules.

PCA Analysis. Before going into the local motions, we examine the large scale motions of the protein by the principal component analysis (PCA) of the covariance matrix of the C_α

dx.doi.org/10.1021/bi300557y | *Biochemistry* 2012, 51, 6238−6245

coordinates. Measured by eigenvalues of PCA, PC 1 and PC 2 (the most dominant PCs) contribute 54.1% and 15.3% respectively to the overall motion (normalized by the trace of the covariance matrix). Together, the 10 most dominant PCs contribute 95% to the overall motion. In Figure 1b, PC 1 and PC 2 represent the top two principal components calculated from a mixture of 140 000 snapshots of the 0H and 100H trajectories (70 000 each). Then the final 70 000 snapshots of each system were projected onto PC 1 and PC 2. The color legend (each color contains 10 000 snapshots, representing 10 ns simulation) shows the time evolution of the two principal components. From Figure 1b, we observed that PC 1 clearly demonstrates that the lipase has a different conformational ensemble when in an aqueous solution than when it is in hexane-containing solvent systems. Here, 0H exhibits a negative PC 1 while all the hexane-containing systems have a positive PC 1. Also, 0H shows more than double the amount of variation along PC 2 compared to the hexane-containing systems. Whether the system is settled down in a free energy landscape basin or not was roughly monitored by the motion of the protein in 10-ns blocks, that is, how conformational ensemble of each time block is different from that of the previous block. Judged by the time evolution of global motions projected onto PCs 1 and 2, we observed that the 0H and 95H systems take roughly 50−70 ns to begin to converge while the 5H and 100H systems take about 20 ns or less to show convergence.

Upon further structural examination (after convergence), the lipase from 0H appears to have a closed channel, while the lipases in the hexane-containing systems have an open channel. For the current setup, it takes tens of nanoseconds for a lipase from the crystal structure conformation to settle down to the closed conformation ensemble when it is immersed in aqueous solution. Interestingly, the systems that take the longest to converge were constructed with water molecules initially placed on the surface of the protein, whereas systems that converge in less than 20 ns were constructed with hexane molecules in the first solvation layer. In addition, from the areas of the final 10 ns color block (gray) in the PCA plot, the flexibility of the lipase in increasing order is 100H, 0H, 95H, and 5H. This indicates that basins of free energy landscape of water-containing systems are flatter which facilitate conformational exploration of the lipase while pure hexane confines this exploration. It would also be interesting to quantify this organic solvent contribution to the energetic roughness[39] of the protein landscape in complex solvent systems in the future.

Flexibility of Lipase Influenced by Solvent Environments. Figure 1c shows a plot of the two-dimensional overall root mean squared deviation (2D-rmsd) of each system. Here the x and y axes represent the mean structures of the 0H and 100H systems, respectively. The 2D-rmsd is calculated from the trajectory of each system and projected onto the average structures of the lipase in 0H and 100H. As expected 0H and 100H systems show a low rmsd value on their respective axes. However, both 5H and 95H show an rmsd greater than 3 for each axis. It is apparent that while each initial lipase structure is identical, the unique protein−solvent interactions in each simulation lead the lipase along a pathway toward a specific local low energy conformation. Remarkably, lipases solvated in the water−oil mixtures seem to converge to similar structural ensembles regardless of the difference of the overall composition of the mixture.

Since we have characterized the global motions of the lipase, we now zoom in on the local aspects of the access channel. First, we examine the local flexibility of the lipase in different solvent environments using the Debye−Waller factor (B-factor) which reveals the locality of an atom and can be calculated by using the mean-square fluctuation, $B = 8\pi^2\langle\Delta r^2\rangle/3$. Figure 1d shows the deviation from the mean at the residue level, calculated from the last 70 ns. The α5 helix (residues 126−147) consistently shows one of the highest B-factor values for all four systems, especially for 0H system. Also, the α5 shows a comparable B-factor in the two mixture systems, 5H and 95H. The systems (0H and 95H) that were constructed with water molecules in the first solvation layer show a similar B-factor for the α8, and the same holds true for the 5H and 100H systems with hexane molecules in the first solvation layer. This increase in fluctuation around the average structure for the α5 in the 0H system is contributed by the transient motion of gate closing, not the equilibrium fluctuation. Figure 1e shows the B-factor for each system calculated from the last 10 ns of the simulation where this transient motion is eliminated. Here we see that the 5H system is most flexible, 95H follows, then 0H, and 100H. This is consistent with the trend observed from the PCA analysis. Again, from PCA, overall rmsd and B-factor analysis, we observed that the rigidity of this protein is increased when it is immersed in hexane. Our observation of lower flexibility in hexane media (than in water) is also consistent with studies performed on another hydrolase system, the crystal structure of chymotrypsin with hexane.[40] Many factors, from specific protein−solvent interactions to a generic hydrophobic solvent effect, may contribute to the origin of this immobilization effect by hexane media. For example, a hexane environment does not provide solvent hydrogen bonds that would otherwise "lubricate" the protein motion.

Gating Motion of the Access Channel. By monitoring the gorge radius, we quantify the solvent-induced gating motions of the lipase. From the crystal structure, this gorge has an ovoid shape of radius 3 Å and dimensions 10 Å × 25 Å.[16] In the four solvated systems with ligand removed, the size and shape of this gorge change to accommodate solvent molecules.

In Figure 2a, the gorge radius is shown as a function of time, from which we observed that the gating motion of the lipase is highly active at the interface (5H and 95H systems). In the 100H system, the gorge radius of the lipase persistently fluctuates around 1 to 2.5 (reaches a maximum of 3 Å), which implies that there is very little structural perturbation on the initial configuration. In contrast, the gorge radius in the 0H system slowly but steadily decreases from 3 to 1 Å. Using simple distance criterion, similar conclusions on gate closing in aqueous simulation of lipases have been reported previously.[14,22] The radius of the gorge in 5H reaches nearly double that of the crystal structure (from 3 to roughly 6 Å), and 95H reaches a gorge radius of about 4 Å. This opening of the gorge is possibly the result of the complementary forces that act on the protein in a complex interfacial environment. We will discuss the opening mechanism in detail below from the movement of the amphiphilic α5 perspective.

The distribution of gorge radius $p(r)$ shown in Figure 2b reveals interesting bimodal distributions, especially for that of the 100H system. The lipase has the highest probability of being in an open-state in 5H (broadest distribution) while least in 0H (narrowest distribution). The 5H and 95H having similar distribution at a larger gorge radius denotes that the lipase favors an open conformation at an interface. On the basis of the

dx.doi.org/10.1021/bi300557y | Biochemistry 2012, 51, 6238−6245

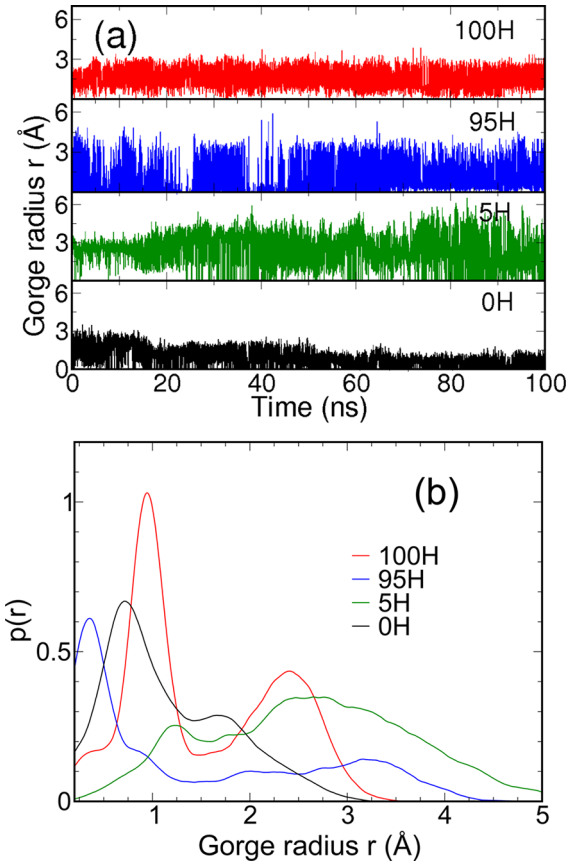

Figure 2. The time series (a) and distribution (b) of the gorge radii of the access channel in different solvent systems. Color notation is identical to that of Figure 1c.

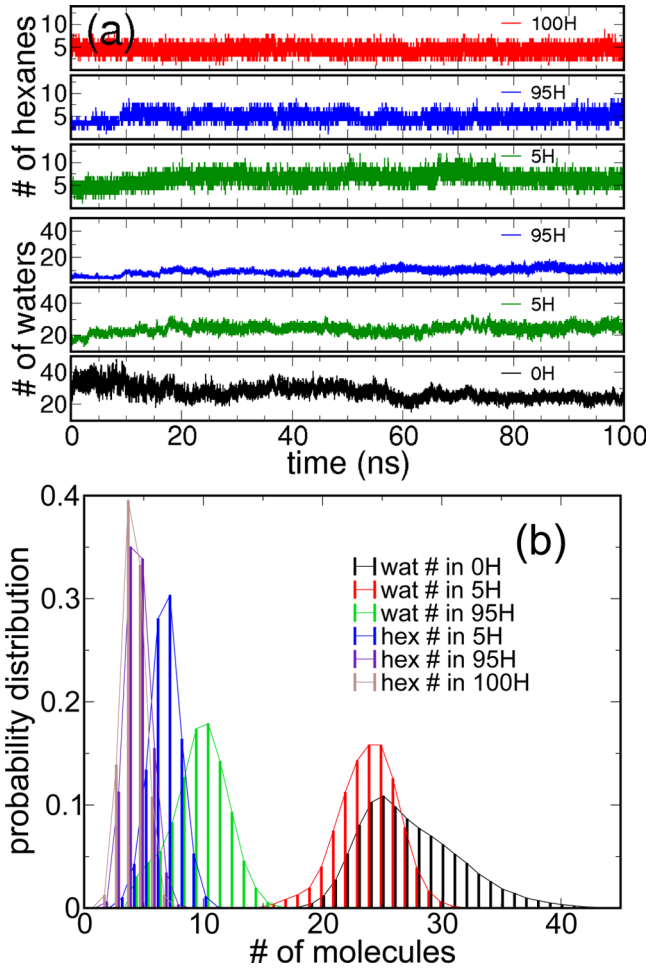

Figure 3. The time series (a) and distribution (b) of the number of solvent molecules in the gorge.

distributions, it appears that an open-gate conformation is most likely achieved when a small amount of organic moiety is present in an aqueous environment.

Solvent Molecules inside the Access Channel. In Figure 3a, we monitor the number of solvent molecules found in the access channel as a function of time. This analysis is done by searching for solvent molecules within a radius of 10 Å from Ser[82]. Note that in the crystal structure the distance from the active site to the mouth of the access channel is about 15 Å. Several other cutoffs greater than 10 Å were tested but yielded significant inclusion of bulk solvent molecules (data not shown). The top three panels in Figure 3a represent the number of hexane molecules found in the gorge throughout the course of the simulation. Notice that each hexane-containing system does allow roughly 5−10 hexane molecules into the gorge, but the 5H system clearly admits the greatest amount of hexane molecules into the gorge, as lipase of 5H exhibits the widest gorge opening (Figure 2). Figure 3b displays the statistics of solvent molecules. Here, the number of hexane molecules in the 5H system shows the widest distribution. This indicates that a significant amount of hexane molecules are moving in and out of the gorge. The relatively constant amount of gorge hexanes in 100H may be correlated to the insignificant change in gorge size (Figure 2). As shown in Figure 3b, 100H has the narrowest distribution of gorge hexane molecules. The 95H system shows an initial increase in the amount of gorge hexanes, but it is less than the amount of hexanes in 5H, as the protein in 95H does not open as wide as that in 5H.

In Figure 3a, the bottom three panels represent the number of water molecules found in the gorge as time evolves. Here, the 0H system initially has the greatest amount of water inside the gorge due to an initial void in the access channel left from the ligand removal. However, the water molecules are squeezed out as the gorge narrows due to its hydrophobic nature. During this process, the lipase in 0H is slowly transformed from an initial open to a closed conformation. The widest distribution of gorge waters in 0H shown in Figure 3b also indicates a substantial amount of water molecules being excluded from the gorge. In agreement with the PCA data (Figure 1), the amount of water becomes relatively stable around the 70 ns mark as the protein relaxes into the close conformation ensemble. Both 5H and 95H show a modest increase in the amount of gorge waters. The 5H system shows more water molecules in the gorge as it has a more open structure. Figure 3 clearly shows that 5H accommodates the highest amount of solvent molecules. Thus, the molecular interface constructed by the gorge solvent molecules can be seen as being vital in the gating mechanism of the access channel.

The Role of the Lid Region in the Mechanism of Interfacial Activation. As previously stated, the lipase regulates gating via the motion of the lid region. This region is defined mainly by four helices: α4 (residues 113−120), α5 (residues 126−147), α6 (residues 155−162), and α8 (residues 210−222). Previous studies have shown that the channel can be

dx.doi.org/10.1021/bi300557y | *Biochemistry* 2012, 51, 6238−6245

closed either by movement of the α4 and α6 helices toward each other or by shifting α5 and α8 closer together.[22] We have found by local rmsd analysis (not shown here) that by a significant magnitude the motions of the other three helices (α4, α6, α8) are negligible compared to that of amphiphilic α5. So, we focus on the relative motion of α5 and α8 and how this constriction is related to the opening and closing of the channel. The distance between α5 (Cα of Ile[159]) and α8 (Cα of His[215]) reported in Figure 4a shows that in the 0H system α5

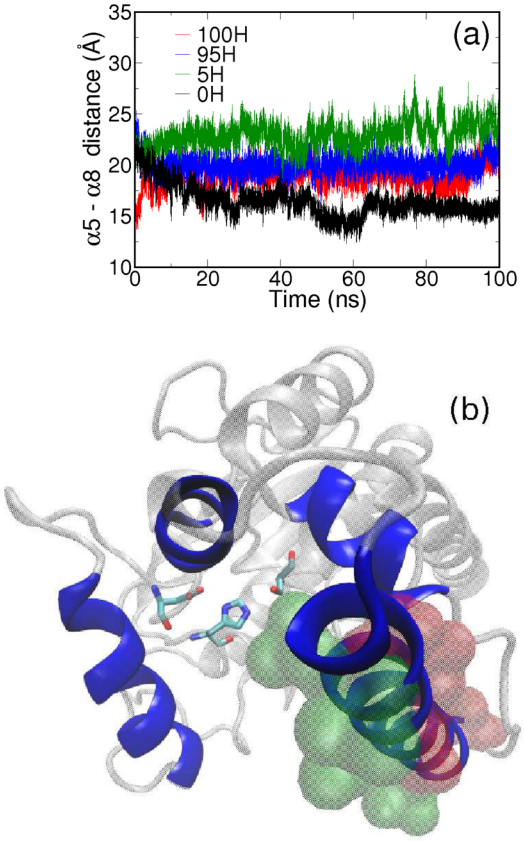

Figure 4. (a) Change in the distance of the helices α5 (Cα of Ile[159]) and α8 (Cα of His[215]) through time in various solvents. Color notation is identical to that of Figure 1c. (b) A top view of the gorge entrance. Helices α4, α5, α6, and α8 are colored in blue. The three residues (stick representation) near the core of the protein are part of the catalytic triad (Ser[82], Asp[229], and His[251]). The green and red shadings indicate the hydrophobic and hydrophilic faces of the α5 helix, respectively.

constricts toward α8 as the simulation proceeds, from roughly 23 Å to 17 Å. Also, it shows that the interhelix distance actually reaches more than 20 Å in all the hexane-containing systems. Here 5H yields both the highest average value and highest maximum value.

The constriction of the lid region in 0H may signify that the closure is driven by the hydrophobicity of the inner "core" face of the amphiphilic α5 (Figure 4b). The interaction of the aqueous solvent and α5 may push the helix inward.[41] Conversely, the highly hydrophobic solvent environment of 100H interacts with α5 differently, and α5 shows no such movement toward α8. Although 5H and 95H are both good candidates for interfacial activation, the 5H system (Figure 3) allows more solvent molecules into the gorge and displaces α5 away from α8. In contrast to the pure systems, the mixtures present the environment for ideal interfacial activation wherein complementary forces may act on the amphiphilic helix.

CONCLUSIONS

Four sets of 100 ns simulations of the lipase were performed in aqueous solution, hydrophobic solvent (hexane), and two water−oil mixtures (5H and 95H) with molecular immiscible interfaces. Because of the long time-scale and unique solvent composition used in these simulations, we are able to quantitatively observe the gating motions of this lipase in detail. We found that the relaxation time is quite long (tens of nanoseconds) for two of the systems that have water placed inside the channel as the initial states (0H and 95H systems). The bottleneck of the gating dynamics seems to be the repelling of water by either constricting the gorge or replacing water with hexane. As supported by both PCA and 2D-rmsd, the lipase assumes distinct conformational states when exposed to different solvent systems studied here. The simulation in pure hexane produces the least structural deviation from the starting conformation. In contrast, the lipase shows the highest amount of structural changes in the aqueous solution.

The lipase exhibits a strong bimodal gorge radius distribution, open and closed states, for system 100H. When in the open state, the lipase yields a persistent gorge radius of 3 Å, while in the 0H system it produces a narrowing gorge radius from 3 to 1 Å as water is squeezed out. In contrast, the two mixture systems (5H and 95H) actually show a remarkable widening of the gorge from 3 to 4−6 Å. The lipase in 5% hexane shows the widest maximum gorge radius of 6 Å.

We believe that the presence of minute organic moiety in a significantly aqueous environment is a very desirable molecular motif for lipase activation. Two interfacial environments (5H and 95H) were created to provide some qualitative features. However, it is far from obtaining a qualitative answer to the optimum mixture and solvent structure to maximize the lipase activity. This question highlights the difficulty of studying protein at immiscible interfaces compared to that in solutions.

Properties obtained here will also facilitate the comparison of lipase conformational dynamics in other organic solvent medias and in high pressure conditions in other studies in the future. These quantitative analyses on lipase conformations and solvent structures provide a mechanism for examining the molecular immiscible interface-activated conformational switch of proteins, especially on the use of an amphiphilic helix (α5 in this case) as the critical component.

AUTHOR INFORMATION

Corresponding Author

*E-mail: tshen@utk.edu, phone: (865)974-4088, fax: (865) 974-6306.

Funding

Q.R.J. acknowledges the PEER graduate training program for funding provided via an NIH grant.

Notes

The authors declare no competing financial interest.

ACKNOWLEDGMENTS

We acknowledge the computational support provided in part by the UT-ORNL Center for Molecular Biophysics, and by an allocation of advanced computing resource (TG-MCB120011) on Kraken at the National Institute for Computational Sciences.

■ ABBREVIATIONS:

PAL, *Pseudomonas aeruginosa* lipase; PCA, principal component analysis; 2D-rmsd, two-dimensional root-mean-square-deviation

■ REFERENCES

(1) Fersht, A. (1999) *Structure and Mechanism in Protein Science: A Guide to Enzyme Catalysis and Protein Folding*, W.H. Freeman, New York.

(2) Klibanov, A. (2001) Improving enzymes by using them in organic solvents. *Nature 409*, 241−246.

(3) Nicolas, J. P. (2003) Molecular dynamics simulation of surfactin molecules at the water-hexane interface. *Biophys. J. 85*, 1377−1391.

(4) Jaeger, K.-E., and Scheidininger, B. (1997) Bacterial lipases for biotechnological applications. *Mol. Catal. 3*, 3−12.

(5) Jaeger, K.-E., Dijkstra, B. W., and Reetz, M. T. (1999) Bacterial biocatalysts: Molecular biology, structure and biotechnological applications of lipases. *Annu. Rev. Microbiol. 53*, 315−351.

(6) Ogino, H. (2008) in *Protein Adaptation in Extremophiles* (Siddiqui, K. S., Thomas, T., Eds.) pp 193−236, Nova Biomedical, Waltham, MA.

(7) Uttatree, S., Winayanuwattikun, P., and Charoenpanich, J. (2010) Isolation and characterization of a novel thermophilic-organic solvent stable lipase from *Acinetobacter baylyi*. *Appl. Biochem. Biotechnol. 162*, 1362−1376.

(8) Theil, F. (1995) Lipase-supported synthesis of biologically active compounds. *Chem. Rev. 95*, 2203−2227.

(9) Schrag, J. D., and Cygler, M. (1997) Lipases and alpha/beta hydrolase fold. *Methods Enzymol. 284*, 85−107.

(10) Jaeger, K.-E., Ransac, S., Dijkstra, B. W., Colson, C., van Heuvel, M., and Misset, O. (1994) Bacterial Lipases. *FEMS Microbiol. Rev. 15*, 29−63.

(11) Eltaweel, M. A., Rahman, R. N., Salleh, A. B., and Basri, M. (2005) An organic solvent-stable lipase from *Bacillus* sp. strain 42. *Ann. Microb. 55*, 187−192.

(12) Nardini, M., and Dijkstra, B. W. (1999) Alpha/beta hydrolase fold enzymes: The family keeps growing. *Curr. Opin. Struct. Biol. 9*, 732−737.

(13) Gilbert, E. J. (1993) Pseudomonas lipases: Biochemical properties and molecular cloning. *Enzyme Microb. Technol. 15*, 634−645.

(14) Trodler, P., Schmid, R., and Pleiss, J. (2009) Modeling of solvent-dependent conformational transitions in Burkholderia cepacia lipase. *BMC Struct. Biol. 9*, 1−13.

(15) Uppenberg, J., Hansen, M., Shamkant, P., and Jones, T. (1994) The sequence, crystal structure determination and refinement of two crystal forms of lipase B from *Candida antarctica*. *Structure 2*, 293−308.

(16) Nardini, M., Lang, D. A., Liebeton, K., Jaeger, K., and Dijkstra, B. W. (2000) Crystal structure of *Pseudomonas aeruginosa* lipase in the open conformation. *J. Biol. Chem. 275*, 31219−31225.

(17) Lang, D., Hofmann, B., Haalck, L., Hecht, H.-J., Spener, F., Schmid, R. D., and Schomburg, D. (1996) Crystal structure of a bacterial lipase from *Chromobacterium viscosum* ATCC 6918 refined at 1.6 Å. *J. Mol. Biol. 259*, 704−717.

(18) Kim, K. K., Song, H. K., Shin, D. H., Hwang, K. Y., and Suh, S. W. (1997) The crystal structure of a triacylglycerol lipase from *Pseudomonas cepacia reveals* a highly open conformation in the absence of a bound inhibitor. *Structure 5*, 173−185.

(19) Tyndall, J. D. A., Sinchaikul, S., Fothergill-Gilmore, L. A., Taylor, P., and Walkinshaw, M. D. (2002) Crystal structure of a thermostable lipase from *Bacillus stearothermophilus* P1. *J. Mol. Biol. 323*, 859−869.

(20) Derewenda, U., Swenson, L., Wei, Y., Green, R., Kobos, P., Joerger, R., Haas, M., and Derewenda, Z. (1994) Conformational lability of lipases observed in the absence of an oil-water interface: Crystallographic studies of enzymes from the fungi *Humicola lanuginosa* and *Rhizopus delemar*. *J. Lipid Res. 35*, 524−534.

(21) Matsumura, H., Yamamoto, T., Mori, T., and Salleh, A. (2007) Novel cation-pi interaction revealed by crystal structure of thermoalkalophilic lipase. *Proteins 70*, 592−598.

(22) Cherukuvada, S., Seshasayee, A., Raghunathan, K., and Pennathur, G. (2005) Evidence of a double-lid movement in Pseudomonas aeruginosa lipase: Insights from molecular dynamics simulations. *PLoS Comput. Biol. 1*, 182−189.

(23) Invernizzi, G., Papaleo, E., Grandori, R., and Lotti, M. (2009) Relevance of metal ions for lipase stability: Structural rearrangements induced in the *Burkholderia glumae* lipase by calcium depletion. *J. Struct. Biol. 168*, 562−570.

(24) Branco, R., Graber, M., Denis, V., and Pleiss, J. (2009) Molecular mechanism of the hydration of *Candida antarctica* lipase B in the gas phase: Water adsorption isotherms and molecular dynamics simulations. *ChemBioChem 10*, 2913−2919.

(25) Barbe, S., Lafaquiere, V., and Andre, I. (2009) Insights into lid movements of *Burkholderia cepacia* lipase inferred from molecular dynamics simulations. *Proteins: Struct., Funct., Bioinf. 77*, 509−523.

(26) Hamid, T., Rahman, R., and Basri, M. (2009) The role of lid in protein-solvent interaction of the simulated solvent stable thermostable lipase from Bacillus strain 42 in water-solvent mixtures. *Biotechnol. Biotechnol. EQ. 23*, 1524−1530.

(27) Karjiban, R., Rahman, M., and Wahab, H. (2009) Molecular dynamics study of the structure, flexibility and dynamics of thermostable L1 lipase at high temperatures. *Protein J. 28*, 14−23.

(28) Karjiban, R., Rahman, M., and Chor, A. (2010) On the importance of the small domain in the thermostability of thermoalkalophilic lipases from L1 and T1: Insights from molecular dynamics simulation. *Protein Pept. Lett. 17*, 1−9.

(29) Peters, G., Toxvaerd, S., and Svendsen, A. (1997) Computational studies of the activation of lipases and the effect of a hydrophobic environment. *Protein Eng. 10*, 137−147.

(30) Jensen, M., Jensen, T., Kjaer, K., Bjornholm, T., Mouritsen, O. G., and Peters, G. H. (2002) Orientation and conformations of a lipase at an interface studied by molecualr dynamics. *Biophys. J. 83*, 98−111.

(31) Ogino, H., Katou, Y., Akagi, R., Mimitsuka, T., Hiroshima, S., Gemba, Y., Doukyu, N., Yasuda, M., Ishimi, K., and Ishikawa, H. (2007) Cloning and expression of gene, and activation of an organic solvent-stable lipase from *Pseudomonas aeruginosa* LST-03. *Extremophiles 11*, 809−17.

(32) Ogino, H., Nakagawa, S., Shinya, K., Muto, T., Fujimura, N., Yasuda, M., and Ishikawa, H. (2000) Purification and characterization of organic solvent-stable lipase from organic solvent-tolerant *Pseudomonas aeruginosa* LST-03. *J. Biosci. Bioeng. 89*, 451−457.

(33) Case, D. A., Darden, T. A., Cheatham, T. E. I., Simmerling, C. L., Wang, J., Duke, R. E., Luo, R., Crowly, M., Walker, R. C., Zhang, W., Merz, K. M., Wang, B., Hayik, S., Roitberg, A., Seabra, G., Kolossvry, I., Wong, K. F., Pasani, F., Vanicek, J., Wu, X., Brozell, S. R., Steinbrecher, T., Gohlke, H., Yang, L., Tan, C., Mongan, J., Hornak, V., Cui, G., Mathews, D. H., Seetin, M. G., Sagui, C., Babin, V., Kollman, P. A. (2008) Amber molecular dymnamics package, AMBER 10 University of California, San Francisco.

(34) Jorgensen, W. L., Chandrasekhar, J., Madura, J. D., Impey, R. W., and Klein, M. L. (1983) Comparison of simple potential functions for simulating liquid water. *J. Chem. Phys. 79*, 926−935.

(35) Phillips, J. C., Braun, R., Wang, W., Gumbart, J., Tajkhorshid, E., Villa, E., Chipot, C., Skeel, R. D., Kale, L., and Schulten, K. (2005) Scalable molecular dynamics with NAMD. *J. Comput. Chem. 26*, 1781−1802.

(36) Smart, O., Neduvelil, J., Wang, X., Wallace, B., and Sansom, M. (1996) HOLE: A program for the analysis of the pore dimensions of ion channel structural models. *J. Mol. Graphics 14*, 354−360.

(37) Lee, P., and Helms, V. (2012) Identifying continuous pores in protein structures with propores by computational repositioning of gating residues. *Proteins: Struct., Funct., Bioinformatics 80*, 421−432.

(38) Xin, Y., Gadda, G., and Hamelberg, D. (2009) The cluster of hydrophobic residues controls the entrance to the active site of choline oxidase. *Biochemistry 48*, 9599−9605.

(39) Johnson, Q., Doshi, U., Shen, T., and Hamelberg, D. (2010) Water's contribution to the energetic roughness from peptide dynamics. *J. Chem. Theory Comput. 6*, 2591−2597.
(40) Yennawar, N. H., Yennawar, H. P., and Farber, G. K. (1994) X-ray crystal structure of gamma-chymotrypsin in hexane. *Biochemistry 33*, 7326−7336.
(41) Breslow, R. (1991) Hydrophobic effects on simple organic reactions in water. *Acc. Chem. Res. 24*, 159−164.